frontiers | Frontiers in Materials

TYPE Original Research
PUBLISHED 20 June 2023
DOI 10.3389/fmats.2023.1210542

OPEN ACCESS

EDITED BY
Raana Sarvari,
Tabriz University of Medical Sciences, Iran

REVIEWED BY
Saleheh Abbaspoor,
Damghan University, Iran
Luo Zheng,
Xiamen University, China

*CORRESPONDENCE
Hadi Tabesh,
hadi.tabesh@ut.ac.ir

RECEIVED 22 April 2023
ACCEPTED 12 June 2023
PUBLISHED 20 June 2023

CITATION
Hosseinzadeh F, Tabesh H and Farzaneh F (2023), Nano drug delivery platform based on thermosensitive PEG-PCL hydrogel encapsulated in silver-bearing micelles and its antifungal activity investigation against vaginal candidiasis. *Front. Mater.* 10:1210542. doi: 10.3389/fmats.2023.1210542

Nano drug delivery platform based on thermosensitive PEG-PCL hydrogel encapsulated in silver-bearing micelles and its antifungal activity investigation against vaginal candidiasis

Fatemeh Hosseinzadeh[1], Hadi Tabesh[1]* and Farah Farzaneh[2]

[1]Department of Life Science Engineering, Faculty of New Sciences and Technologies, University of Tehran, Tehran, Iran, [2]Preventative Gynecology Research Center, Shahid Beheshti University of Medical Sciences, Tehran, Iran

Introduction: Vaginal candidiasis is a genital mucosal disease. Polymeric micelles (PMs) utilization due to improved solubility and low bioavailability of hydrophobic drugs e.g. clotrimazole is of interest. Silver nanoparticles could be applied to enhance antifungal properties. Loading PMs in injectable thermosensitive hydrogels by rapid distribution across vaginal walls improves the bioavailability of the drug and provides suitable therapeutic efficiency for drug delivery systems.

Method: PCL-PEG-PCL (LGL) and PEG-PCL-PEG (GLG) copolymers were characterized by FTIR, HNMR, and GPC. Zeta potential and Size of synthesized PMs were determined by EMSA and DLS technics and morphological examination of PMs was conducted by FESEM and TEM. Silver-bearing polymeric micelles (PM-Ag) were characterized by DLS and LDE technics. EDX and UV-VIS spectroscopy confirmed silver nanoparticles' binding to PMs. Thermosensitive GLG hydrogel was considered a carrier for PM-Ag.

Results: Encapsulation efficiency and drug loading content of micelles were calculated 64.53% and 14.6% respectively. The diameter and zeta potential of PMs were measured 166 ± 1.73 nm±SD and −6.26 ± 0.3 mV±SD and after silver-bearing it reached 197 ± 2.29 nm±SD and −5.38 ± 0.45 mV±SD respectively.

Discussion: The biocompatibility of samples was investigated by MTT assay and the results indicated that up to a concentration of 125 µg/mL, the relative cell viability percentage exceeded 80%. Therefore, by considering the acceptable antifungal activity of the samples against *C. Albicans*, the designed drug delivery system is capable of sustained drug release over a specified period.

KEYWORDS

polymeric micelle, silver nanoparticle, vaginal drug delivery, antifungal drug, thermosensitive hydrogel

1 Introduction

One of the most common mucosal infections in females is vaginal candidiasis (VC), which is caused by *candida* species such as *Candida* Albicans. It is the second most prevalent mucosal infection after bacterial vaginosis (Johal et al., 2016). Empirical evidence suggests that VC affects a substantial number of women of reproductive age, with estimates ranging from 70%–75%. Additionally, the likelihood of recurrence is anticipated to be in the range of 40%–45%. VC commonly exhibits symptoms such as pruritus, burning, erythema, and edema (Brandolt et al., 2017; Willems et al., 2020). Clotrimazole formulations have been recognized as efficacious pharmacotherapy for this ailment. However, the low biodegradability and limited bioavailability of clotrimazole limit its therapeutic potential. To mitigate these issues, the utilization of nanosystems, such as polymeric micelles, represents a promising strategy to enhance clotrimazole's solubility and bioavailability. Moreover, incorporating silver nanoparticles into these nanosystems could further potentiate the antifungal properties of clotrimazole, thereby augmenting the overall therapeutic efficacy of this pharmacological intervention.

Clotrimazole, an imidazole derivative with potent antimycotic properties, is primarily utilized topically to manage fungal and dermatophyte infections of the mouth, vagina, and skin. Despite its effectiveness, clotrimazole's antifungal activity is hindered by its poor water solubility. This challenge has been addressed through the utilization of various formulations, including nano-based structures, to enhance clotrimazole's bioavailability and efficacy (Santos et al., 2013; Tonglairoum et al., 2017). For the intended purpose, several nano-based systems such as nanocapsules (Santos et al., 2014), nanostructured lipid carriers (NLC) (Nogueira et al., 2022), solid lipid nanoparticles (SLN) (Cassano et al., 2016), liposomes (Abdellatif et al., 2020), nanoemulsions (Soriano-Ruiz et al., 2019), and polymeric micelles (Tonglairoum et al., 2017; Kareem et al., 2019; Catenacci et al., 2020; Albayaty et al., 2021) have been utilized.

Amphiphilic copolymers, comprising both hydrophilic and hydrophobic segments, have gained significant attention as potential nanocarriers. Through self-assembly, these copolymers could form polymer-based amphiphilic nanocarriers with tunable morphology and shape in aqueous solutions. By regulating the balance between the hydrophilic and hydrophobic segments, the synthesis of diverse micelles and vesicles becomes a possibility. Such nanocarriers hold great promise for various applications in drug delivery and biomedicine (Lombardo et al., 2015; Li et al., 2020). Micelle nanocarriers derived from the self-assembly of amphiphilic copolymers at or above critical micelle concentration represent appropriate carriers for encapsulation hydrophobic agents. The core of the micelles can be composed of various polymeric blocks, such as polypropylene glycol, polyesters like PLA (polylactic acid), PCL (polycaprolactone), PLGA (polylactic co glycolic acid), polyamino acids, and lipids (Biswas et al., 2016; Cabral et al., 2018). The hydrophobic core of the micelles serves as the primary site for entrapping lipophilic active ingredients, leading to improved solubility and bioavailability of hydrophobic drugs. The hydrophilic shell of the micelles concurrently creates a stabilizing interface between the two phases, namely, the hydrophobic core and aqueous medium. This interface enhances colloidal stability and effectively prevents undesired interactions with other components (Lombardo et al., 2019). PVP (Polyvinylpyrrolidone), PNIPAm (poly(N-isopropyl acrylamide), PHPMA (Poly(N-(2-hydroxypropyl)methacrylamide), and PEG (polyethylene glycol) are among the nonionic and hydrophilic polymers that are frequently employed in the hydrophilic shell of micelles. PEG is the most commonly used hydrophilic block for the micelle shell due to its high solubility in aqueous media and diverse organic solvents, which provides flexibility in various preparation methods. Moreover, its non-toxicity, low immunogenicity, minimal interaction with other biological components of the body, and ease of biodistribution make it an ideal choice for micelle formulation (Miyata et al., 2011).

The hydrophobic and semi-crystalline polymer, poly(ε-caprolactone) (PCL), consists of repeating units of five non-polar methylene groups and a relatively polar ester group. The polymer is synthesized through the ring-opening polymerization method using ε-caprolactone monomers. Due to its high degree of crystallinity and hydrophobicity, modification of PCL with polyethylene glycol (PEG) to form PCL-PEG copolymers has been proposed (Wei et al., 2009). Several studies have explored the use of PCL-PEG-PCL (LGL) amphiphilic copolymers in the synthesis of micelle nanocarriers containing lipophilic drugs (Gou et al., 2009; Grossen et al., 2017).

Silver nanoparticles (AgNPs) are a type of inorganic nanocarrier that exhibit antibacterial effects against various types of bacteria, including Gram-positive and Gram-negative bacteria. Moreover, AgNPs have demonstrated antifungal properties against *Candida* species. In a study conducted by Panasek et al., it was found that AgNPs at concentrations of approximately 1 mg/L exhibit noteworthy antifungal activities against *Candida* species. Furthermore, the study revealed that these nanoparticles do not induce any cytotoxic effects on human fibroblast cells. These findings suggest that AgNPs could be a potential therapeutic agent for controlling *Candida* infections without causing harm to human cells (Panáček et al., 2009).

Several studies have demonstrated the synergistic antibacterial effects resulting from the combination of silver nanoparticles with antibiotics such as vancomycin, amoxicillin, penicillin G, ampicillin, kanamycin, and erythromycin (Lee and Jun, 2019; Mikhailova, 2020). Moreover, incorporating silver nanoparticles into support materials like polymeric micelles has been instrumental in minimizing aggregation, leading to enhanced antibacterial and antifungal properties (Huang et al., 2017).

The combined strategy of loading nanocarriers into hydrogels has garnered significant attention across various research disciplines. Notably, thermosensitive hydrogels have emerged as a promising candidate for vaginal drug delivery owing to their sol-gel phase transition properties. These hydrogels exhibit a unique property of transitioning from a free-flowing sol state at low temperatures to a gel-like state at 37°C, providing sustained drug release with adjustable kinetics while offering ease of use and prolonged drug residence time. Moreover, the incorporation of nanocarriers in these hydrogels offers reduced leakage and enhanced efficacy, thereby reducing the frequency of administration (Taurin et al., 2018). PEG-PCL-PEG (GLG) is a hydrogel that possesses biodegradability, amphiphilicity, and thermosensitivity, rendering it an attractive material for use in diverse biomedical applications (Gong et al.,

2007). In a study conducted by Frank, it was indicated that the incorporation of polymeric nanocapsules into mucoadhesive semi-solid formulations can effectively augment adhesion and drug diffusion through the vaginal mucosa. This innovative approach holds immense promise for the development of novel therapeutic strategies that can effectively combat a wide range of gynecological disorders (Frank et al., 2017).

Extensive research has been conducted on the use of the vaginal route for pharmacological applications. Compared to the oral route, the vaginal route offers several advantages such as the elimination of hepatic first-pass metabolism, the absence of drug interactions, and the prevention of drug destruction in the gastrointestinal tract. As a result, vaginal drug delivery allows for the possibility of loading lower doses of drugs, which can reduce the occurrence of side effects. Additionally, for drugs targeting the female reproductive system, the use of the vaginal route can lead to higher drug concentrations and improved effectiveness (Ensign et al., 2014; Das Neves et al., 2015). Facchinatto et al. designed chitosan nanoparticles (Clt-NPs) loaded with clotrimazole as a topical treatment for vulvovaginal candidiasis. The Clt-NPs were found to have proper selectivity index values for clinical isolates of *Candida* spp. Similarly, Takahashi and his colleagues synthesized a silver-decorated PVCL-PVA-PEG graft copolymer that demonstrated high antibacterial activity as a drug delivery system effective against biofilm infections (Facchinatto et al., 2021; Takahashi et al., 2021). Considering all of these findings, there remains a gap in the development of a robust drug delivery system capable of loading temperature-sensitive hydrogel with polymeric micelles containing silver nanoparticles, and evaluating its therapeutic efficacy. The main objective of this study focuses on countering *Candida* albicans fungal infection using a PCL-PEG-PCL triblock copolymer composed of an inner PCL core and an outer PEG shell. By encapsulating clotrimazole within the hydrophobic core and decorating the shell with silver nanoparticles, an effective antifungal approach is achieved. Initially, the PCL-PEG-PCL triblock copolymer is synthesized via ring-opening polymerization. Subsequently, polymeric micelles (PMs) are formed using the nano-precipitation method, enabling the simultaneous loading of clotrimazole into the core. The micelles are chemically modified to incorporate silver nanoparticles onto their surface. Silver-beared clotrimazole-loaded micelles are then loaded into the PEG-PCL-PEG hydrogel. This drug delivery system enhances biocompatibility, solubility, and clotrimazole efficacy. Furthermore, the presence of silver nanoparticles contributes to the augmented antifungal properties. The adhesive properties of the PEG-PCL-PEG hydrogel facilitate increased drug diffusion and sustained drug release, thereby prolonging the drug's residence time. This system could prove to be an ideal choice for releasing clotrimazole and silver nanoparticles topically.

2 Materials and methods

2.1 Materials

Polyethylene glycol (PEG) (M_n = 6,000 and 4,000 Da), ε-caprolactone (CL), stannous octoate ($Sn(oct)_2$), Poly(ethylene glycol) methyl ether (mPEG) (M_n = 550 Da), Hexamethylene diisocyanate (HMDI), Silver nitrate ($AgNO_3$), Sodium borohydride ($NaBH_4$), Toluene, Dimethyl sulfoxide (DMSO), Dimethylformamide (DMF) and Dulbecco's Modified Eagle Medium (DMEM) were purchased from Merck (Merck and Co., Inc., Darmstadt, Germany). Clotrimazole and Yeast extract peptone dextrose (YPD) agar were obtained from Sigma–Aldrich (Sigma–Aldrich Chemical Co., St. Louis, MO, United States). All solvents were analytical grade. mPEG was dried by azeotropic distillation method using toluene as previously defined by Kim et al., 2004.

TABLE 1 Chemical structure of LGL and GLG copolymers.

Sample name	Triblock copolymer	PEG MW	PCL/PEG[a]
LGL	PCL_{5000}-PEG_{6000}-PCL_{5000}	6,000	1.67:1
GLG	PEG_{550}-PCL_{2200}-PEG_{550}	550	2:1

[a]Feeding ratio.

2.2 Synthesis of LGL and GLG triblock copolymers

In the pursuit of synthesizing triblock copolymers, we utilized two different molecular weights of PEG, resulting in the formation of three distinct variations: PCL_{5000}-PEG_{6000}-PCL_{5000}, PCL_{4000}-PEG_{4000}-PCL_{4000}, and PCL_{6000}-PEG_{4000}-PCL_{6000}. These copolymers underwent extensive analysis through HNMR, FTIR, and GPC techniques. Subsequently, the copolymers were employed for the construction of micelles, which were evaluated in terms of size distribution, zeta potential distribution, and morphological structures. After a comprehensive assessment, PCL_{5000}-PEG_{6000}-PCL_{5000} (LGL) was chosen as the final structure for further investigation. The hydrogel synthesizing was followed by PEG_{550}-PCL_{2200}-PEG_{550} (GLG) triblock copolymer construction by employing mPEG with a molecular weight of 550 Da. The characterization tests conducted on this copolymer confirmed its attainment of the desired properties.

LGL copolymer was synthesized based on a method adapted from Gou et al. using ε-caprolactone ring-opening polymerization by PEG initiation in the presence of stannous octoate (Gou et al., 2008). By considering a specific amount of PEG (6,000 Da), the required volume of ε-caprolactone was calculated according to the defined stoichiometry relation. PEG was transferred to a 50 cc three-necked volumetric flask followed by adding 3 mL of Dimethylformamide to dissolve it. The calculated amount of ε-caprolactone was then added to the flask and the reaction was carried out under N_2 atmosphere at 130 °C. Stannous octoate was applied along with the temperature rising. After temperature stabilization, the system was sealed completely to proceed with polymerization for 24 h. When the polymerization reaction was accomplished, the purification of obtained polymers was followed by precipitation in cold diethyl ether after being dissolved in dichloromethane. The precipitates were washed several times with DI water before being dehumidified under reduced pressure using a vacuum oven YHV 150X8D (Yaranfurnace Co., Tehran, Iran). GLG copolymer was polymerized according to a two-step reaction (Gong et al.) (Gong et al., 2007; Hwang et al., 2020). Briefly, at first, mPEG-PCL diblock copolymer was synthesized by ring-opening

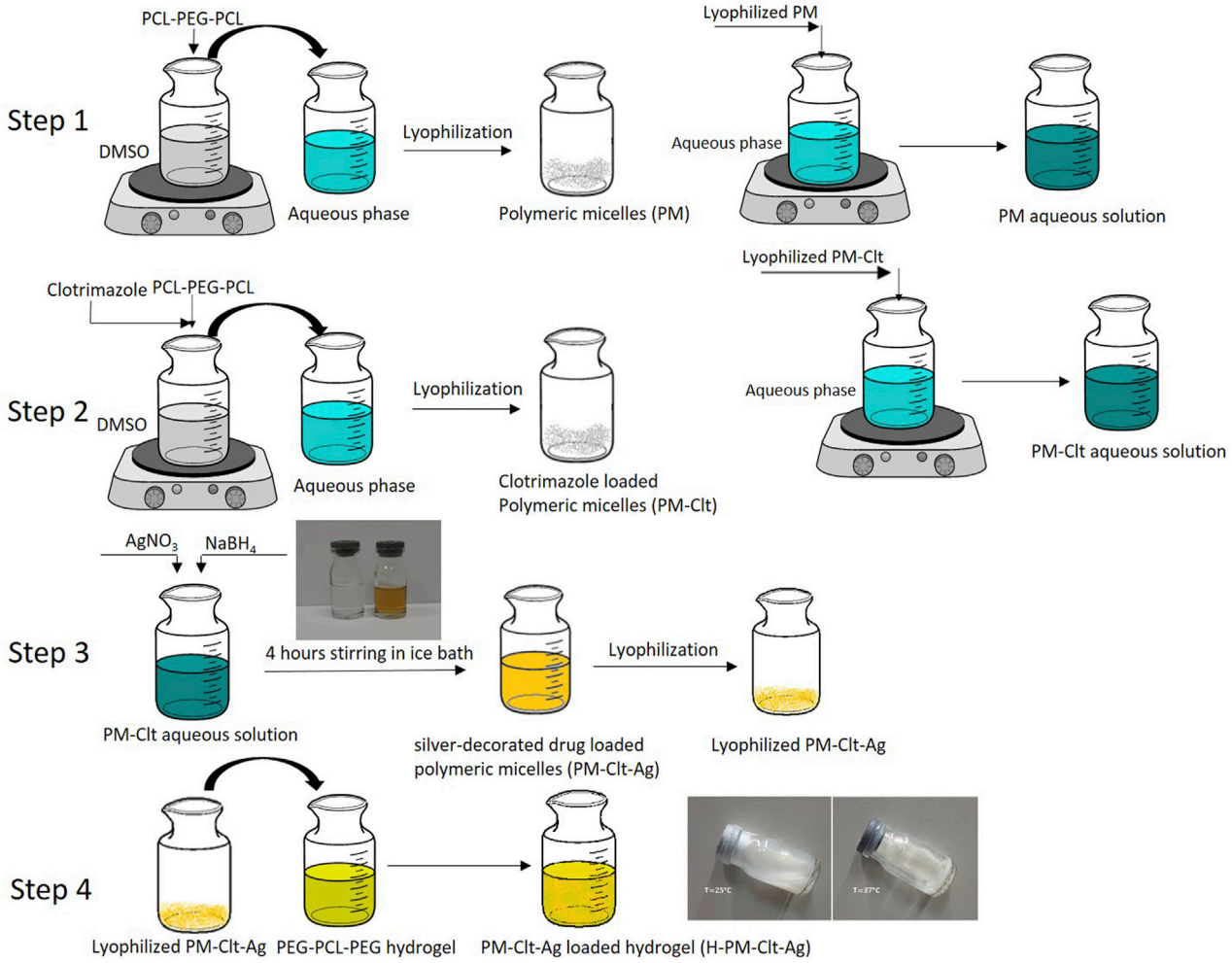

FIGURE 1
Schematic illustration of the Ag-beared polymeric micelle loaded in hydrogel.

polymerization of ε-caprolactone initiated by mPEG (Mn = 550) using ($Sn(oct)_2$) as the catalyst. In the next step, PEG-PCL-PEG copolymer was obtained as a result of mPEG-PCL diblock copolymer coupling by HMDI. The purification of the obtained polymer was performed as above mentioned in the LGL synthesis process. The chemical structure of copolymers has been presented in Table 1.

2.3 Preparation of micelles

Four different micelles including polymeric micelles (PM), clotrimazole-loaded polymeric micelles (PM-Clt), silver-bearing polymeric micelles (PM-Ag), and clotrimazole-loaded Ag micelles (PM-Clt-Ag) were synthesized according to the following methods. In step 1, to produce PM by the nanoprecipitation method (Gou et al., 2009), 20 mg of LGL was dissolved in 1 mL DMSO forming an organic phase. The organic phase was then poured dropwise to 10 mL of aqueous phase while under moderate mechanical stirring. As a result of the diffusion of DMSO in the aqueous phase, LGL block copolymers self-assembled into micelles that featured PCL hydrophobic cores and PEG hydrophilic shells. Following this synthesis, PM solution dialysis was conducted against DI water for 48 h in order to remove DMSO. Finally, the product PM was shaped into a white powder form through drying and vacuum conditions using freeze dryer (Operon, Gyeonggi-do, South Korea).

In step 2, the preparation of PM-Clt was achieved using a similar method. Specifically, a solution containing 7.5/20 (wt/wt) clotrimazole/copolymer in 1 mL DMSO was introduced into 10 mL of an aqueous phase. As a result, LGL block copolymers underwent self-assembly into micelles, with their hydrophobic core effectively entrapping the clotrimazole in an aqueous environment. To eliminate any residual DMSO, the PM-Clt solution was dialyzed against DI water for 48 h. Finally, the PM-Clt solution was subjected to vacuum drying, ultimately yielding PM-Clt lyophilized powder.

The process of preparing PM-Ag involves the use of chemical synthesis in step 3. Initially, a micellar solution with a concentration of 1.25 mg/mL is prepared, and then a solution of $AgNO_3$ with a concentration of 2 mg/mL is added to it while stirring. After a minute of stirring at room temperature in a dark place, 100 μL of 2 mg/mL $NaBH_4$

is introduced into the mixture, which causes the solution to turn yellow instantly. The mixture is then allowed to reduce for 4 hours, after which it is purified using a dialysis bag for 48 h. To prepare PM-Clt-Ag, the same procedure is followed, but with the addition of PM-Clt-Ag powder, which is obtained by lyophilizing the solution. In step 4, The H-PM-Clt-Ag is prepared by dissolving 2 mL of PM-Clt-Ag solution in a specified amount of hydrogel. The Schematic of these processes has been illustrated in Figure 1.

2.4 Polymer characterization

The identification of functional groups in LGL and GLG copolymers was achieved using Tensor 27 FTIR (Bruker Inc., Massachusets, United States) and INOVA 500 MHz HNMR (Bruker Inc., Massachusets, United States). To predict the molecular weights of the synthesized copolymers, HNMR spectra were utilized. Additionally, GPC Breeze QS HPLC (Waters Corp, Massachusets, United States) was used to determine the weight-average molecular weight (M_w), number-average molecular weight (M_n), and weight distribution of the copolymers.

2.5 Characterization of micelles

In order to obtain an accurate assessment of synthesized nanoparticles, a variety of equipment was utilized. To determine the mean particle size and polydispersity index, the Dynamic Light Scattering SZ-100 DLS (Horiba, LTD., Kyoto, Japan) was utilized. This same equipment was also used in measuring the nanoparticle zeta potential in water through the Laser Doppler Electrophoresis (LDE) technique. Furthermore, the surface morphology of the nanoparticles was meticulously examined using the Field Emission Scanning (FESEM) method, utilizing the Mira FESEM equipment (TESCAN, Brno, Czech Republic). In addition, the EM 208S Transmission Electron Microscopy (TEM) (Philips, Amsterdam, Netherlands) was employed to investigate the morphological characteristics of the nanoparticles which provided further insights into their properties.

To determine the encapsulation efficiency (EE) and drug loading content (DL) of micelles, a lyophilized powder of the micelles was dissolved in acetonitrile. Using the calibration curve of the drug in acetonitrile, the concentration of clotrimazole in the solution was determined through NanoDrop 2000/2000c Ultraviolet-visible (UV-vis) spectroscopy (Thermo Fisher Scientific Inc., Massachusetts, United States) at a wavelength of 230 nm. With the total amount of drug in the micelles, Eqs 1, 2 could be used to calculate DL (%) and EE (%), respectively. This methodology allowed for an accurate determination of EE and DL values for the micelles.

$$\text{Drug loading content } (\%) = \frac{\text{Drug weight in nanoparticle}}{\text{Prepared nanoparticle weight}} \times 100 \quad (1)$$

$$\text{Encapsulation efficiency } (\%) = \frac{\text{Drug weight in nanoparticle}}{\text{Drug weight in the feed}} \times 100 \quad (2)$$

The SZ-100 instrument was utilized to carry out size and zeta potential analyses on PM-Ag, which were subsequently compared with those of silver-free polymeric micelles. In addition, the absorbance spectra of PM-Ag were measured using UV-vis spectrophotometry over a wavelength range of 200–600 nm. Energy-dispersive X-ray (EDX) spectroscopy and elemental mapping analysis was implemented using Mira FESEM to verify the presence of structurally incorporated Ag nanoparticles on micelles. Furthermore, inductively Coupled Plasma Mass Spectroscopy (ICP-MS) was performed via Vista-MPX (Varian Inc., California, United States) to accurately measure the concentration of silver nanoparticles that were released from the micelles.

2.6 Clotrimazole release profile

The *in vitro* release profile of clotrimazole from PM-Clt was identified using a diffusion technique. Specifically, 2 mL of the PM-Clt solution was placed into a 12,400 Da molecular weight cutoff dialysis bag and immersed in 10 mL of 10 mM PBS/ethanol at pH 7.30. Ethanol was used to maintain the sink condition during the experiment. The mixture was kept at 37 °C and shaken steadily throughout the experiment. At predefined intervals, 3 mL of release medium was replaced with fresh buffer. The amount of released drug was measured using UV-vis spectroscopy at 230 nm. All drug release values were measured three times and their mean values were reported.

To determine clotrimazole release from H-PM-Clt-Ag, 2 mL of H-PM-Clt-Ag sample was transferred into a 5 mL Eppendorf tube and allowed to incubate for 12 h at 37 °C until a stable gel was formed. Then, the gel was immersed in a solution consisting of 2 mL 10 mM PBS/ethanol at a pH of 7.3 and placed in a shaking incubator that was maintained at 37°C and 100 rpm. At predefined intervals, 1 mL of release medium was removed and substituted with fresh medium. The removed release medium was then centrifuged at a rate of 10,000 rpm for 10 min, following which the supernatant absorption was measured using UV-vis spectroscopy at a wavelength of 230 nm.

2.7 Cytotoxicity assay

The cytotoxicity assessment of PM, PM-Ag, PM-Clt, PM-Clt-Ag, and H-PM-Clt-Ag against HEK293T human embryonic kidney cells was carried out using the 3-(4,5-dimethythiazol-2-yl)-2,5-diphenyltetrazolium bromide (MTT) assay. To accomplish this, cells were cultured in DMEM medium on 96-well plates at a density of 10^4 cells per well in a 5%–95% CO_2-O_2 incubator at 37 °C. Subsequently, various dilutions of samples ranging from 1 to 500 in the cell culture medium were prepared and 100 µL of diluted samples were poured into each well after 24 h of culturing the cells. In the control group, normal saline was employed. Following 48 h, a 100 µL of 0.5 mg/mL MTT was added to each well that was kept in a dark compartment and incubated for 4 h at 37 °C. The MTT-containing medium was then substituted with 100 µL of 0.1 M DMSO, which was then placed on a shaker for 20 min while covered to prevent exposure to light. Finally, the absorption of the samples was measured using DNM-9602 microplate reader (Drawell Scientific Instrument Co., Ltd., Shanghai, China) at 570 nm, and the cell viability percentage was determined by calculating the ratio of the live cells number to the control cells.

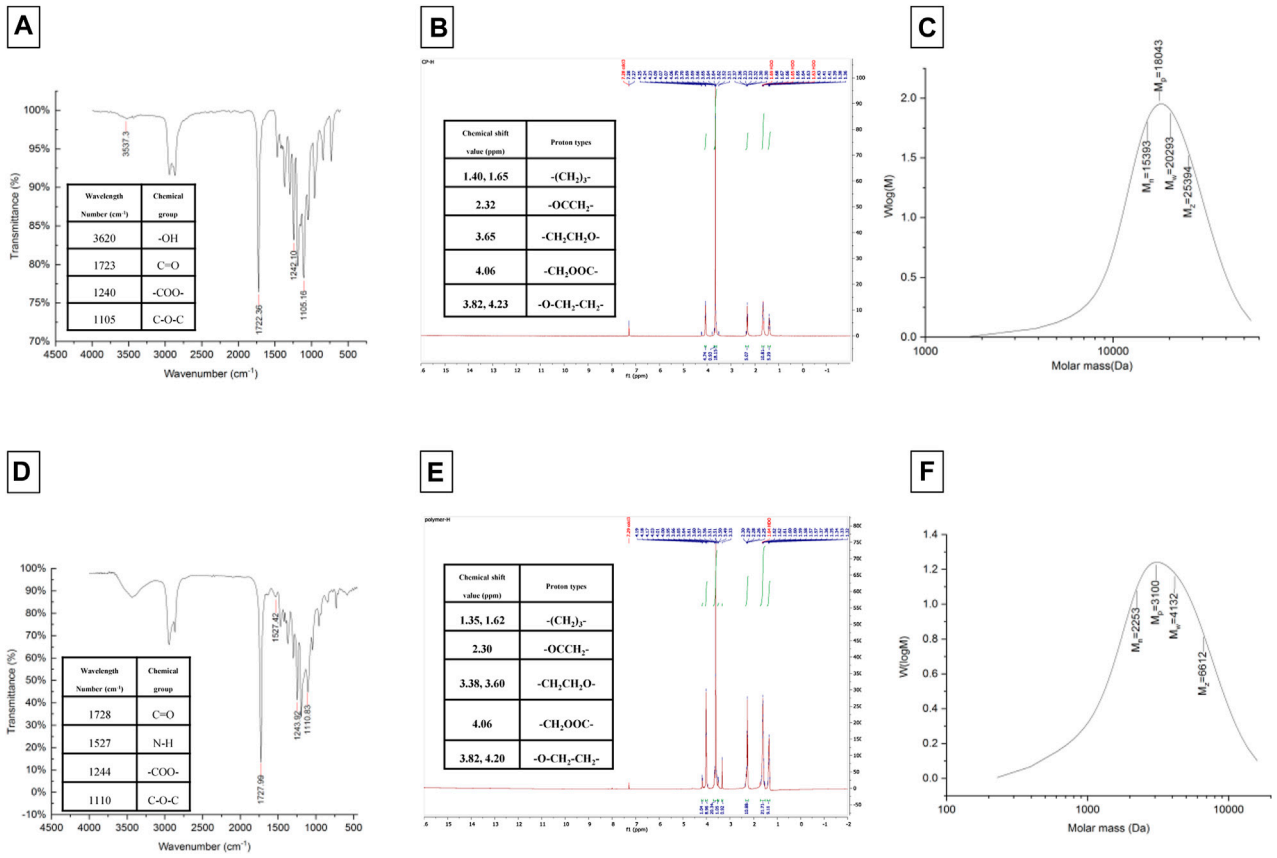

FIGURE 2
FTIR and HNMR spectrums, and GPC chromatogram of LGL **(A–C)** and GLG **(D–F)** copolymers.

2.8 Antifungal activity

Antifungal activity against *Candida* albicans was studied according to standardized protocol M27-A2, CLSI. First, the fungus was cultured on the YPD agar medium and incubated at 35 °C for 48 h. Subsequently, the fungal colony obtained after growth was used to prepare a *candida* suspension. To achieve the desired concentration of 1.0×10^3 cells/mL, a colony of 48-h culture was added to 1 mL of sterile saline and homogenized in a vortex mixer for 15 s to obtain a suspension. By setting the cell density equivalent to a standard 0.5 McFarland scale (1.0×10^6 cells/mL) using spectrophotometry at a wavelength of 530 nm, dilution was performed by withdrawing 5 µL from a 5 mL sterile saline tube and adding 5 mL of 1.0×10^6 cells/mL suspension. The resulting suspension had a concentration of 1.0×10^3 cells/mL. To determine the growth inhibition concentrations, 100 µL of diluted samples in the medium was poured into wells 1 to 10 of a 96-well plate. The samples tested included PM, PM-Ag, PM-Clt, PM-Clt-Ag, and H-PM-Clt-Ag. Hence, 100 µL of fungal suspension was added to all wells except the negative control well. Wells 11 and 12 served as positive (medium + fungal suspension) and negative (medium) controls, respectively. Incubation of the plate for 48 h at 35°C was then carried out. The amount of growth inhibition of different sample concentrations was determined by calculating the difference between the mean absorption of three replicates of each concentration and positive control absorption divided by positive control absorption. The minimum inhibitory concentration was defined as the lowest sample concentration at which the growth was inhibited.

3 Results

3.1 Characterization of triblock copolymers

The synthesis of amphiphilic copolymers of LGL was accomplished by utilizing the ring-opening polymerization method with ε-caprolactone monomers, PEG as an initiator, and stannous octoate as a catalyst. The process for creating the GLG copolymer occurred in two stages: first, the synthesis of PEG-PCL diblock copolymer, followed by obtaining the triblock copolymer using a coupling agent. The chemical structure characterization of the copolymers was determined through FTIR, HNMR, and GPC analyses, which are depicted in Figure 2.

3.2 Characterization of micelles

The values of size, and zeta potential distribution of PM and PM-Ag solutions were determined through the utilization of DLS and laser doppler electrophoresis techniques. The measurements for the average hydrodynamic diameter (d_h) and zeta potential of PM before undergoing silver-bearing treatment were conducted, yielding 166 ±

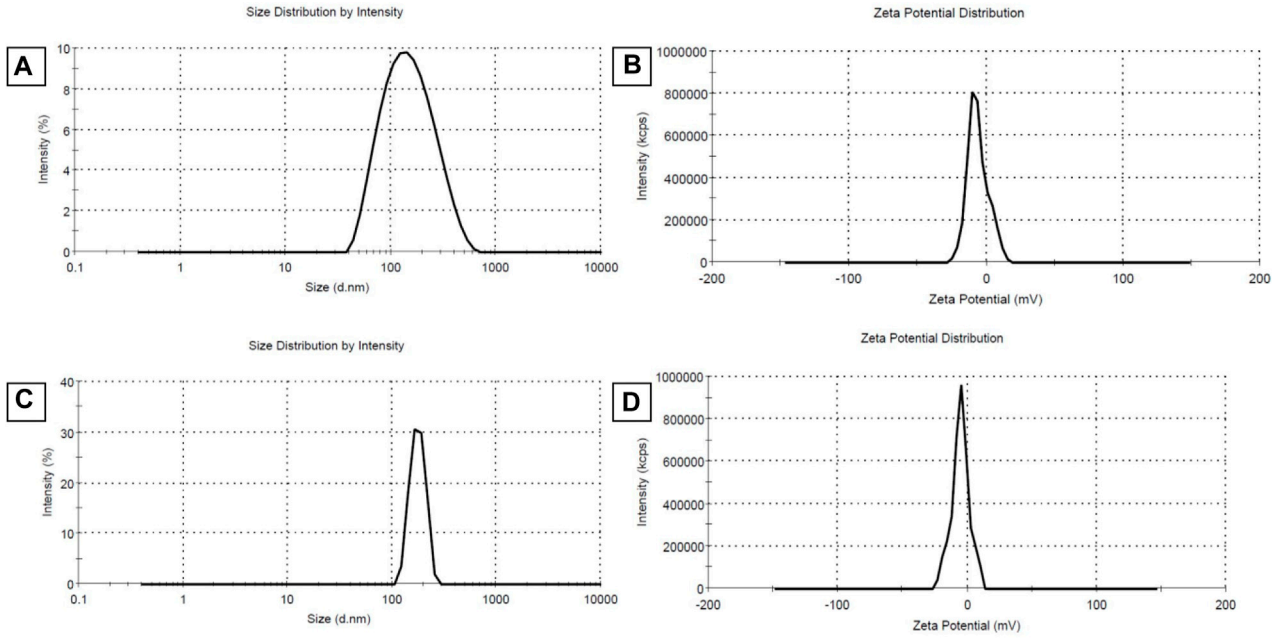

FIGURE 3
Average hydrodynamic diameter (d_h) (size distribution) and zeta potential distribution of Polymeric micelles (PM) **(A,B)** and Silver-beared polymeric micelles (PM-Ag) **(C,D)** respectively.

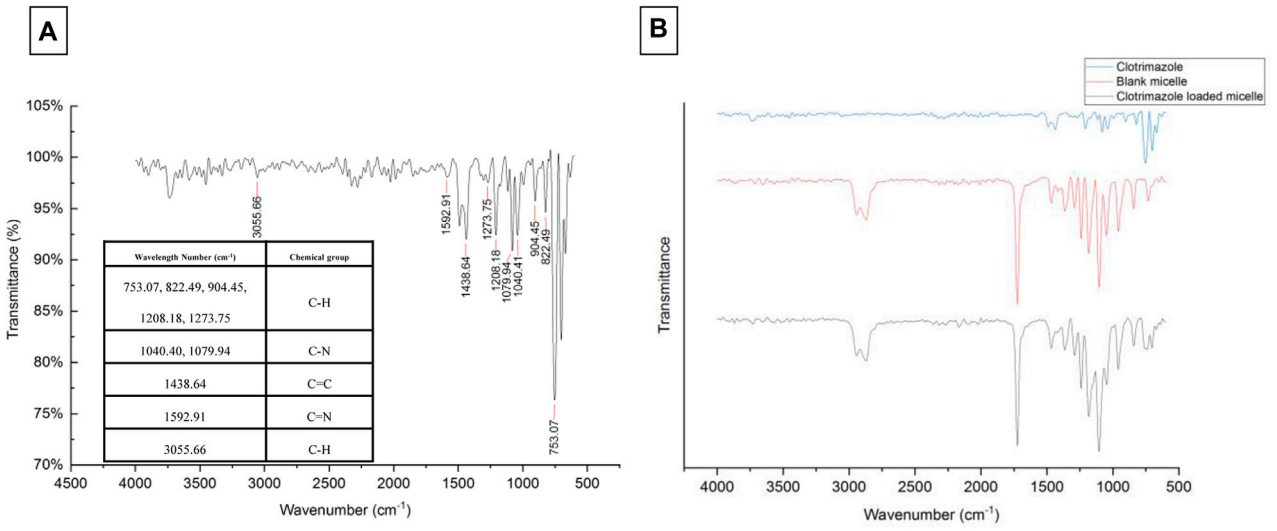

FIGURE 4
Clotrimazole FTIR spectrum with wavelength numbers and corresponding chemical groups **(A)** and comparison of clotrimazole, blank micelle, and clotrimazole-loaded micelle FTIR spectrum **(B)**.

1.73 nm and −6.26 ± 0.3 mV, respectively. After silver-bearing treatment, said values were increased to 197 ± 2.29 nm and −5.38 ± 0.45 mV respectively. The presentation of the size and zeta potential distribution diagram of PM and PM-Ag was completed via Figure 3. The clotrimazole FTIR spectrum with wavelength numbers and corresponding chemical groups besides the comparison graph related to clotrimazole, blank micelle, and clotrimazole-loaded micelle was presented in Figures 4A, B.

The morphology of micelles was assessed through FESEM and TEM imaging. Figures 5A–C depicts FESEM images of micelles captured at resolutions of 1 μm, 500 nm, and 300 nm respectively, while Figure 5D illustrates the morphology of micelles at a resolution of 50 nm as determined by TEM analysis. The spherical shape observed for the micelles, as depicted in Figure 5, is consistent with the particle diameter as determined through DLS data analysis.

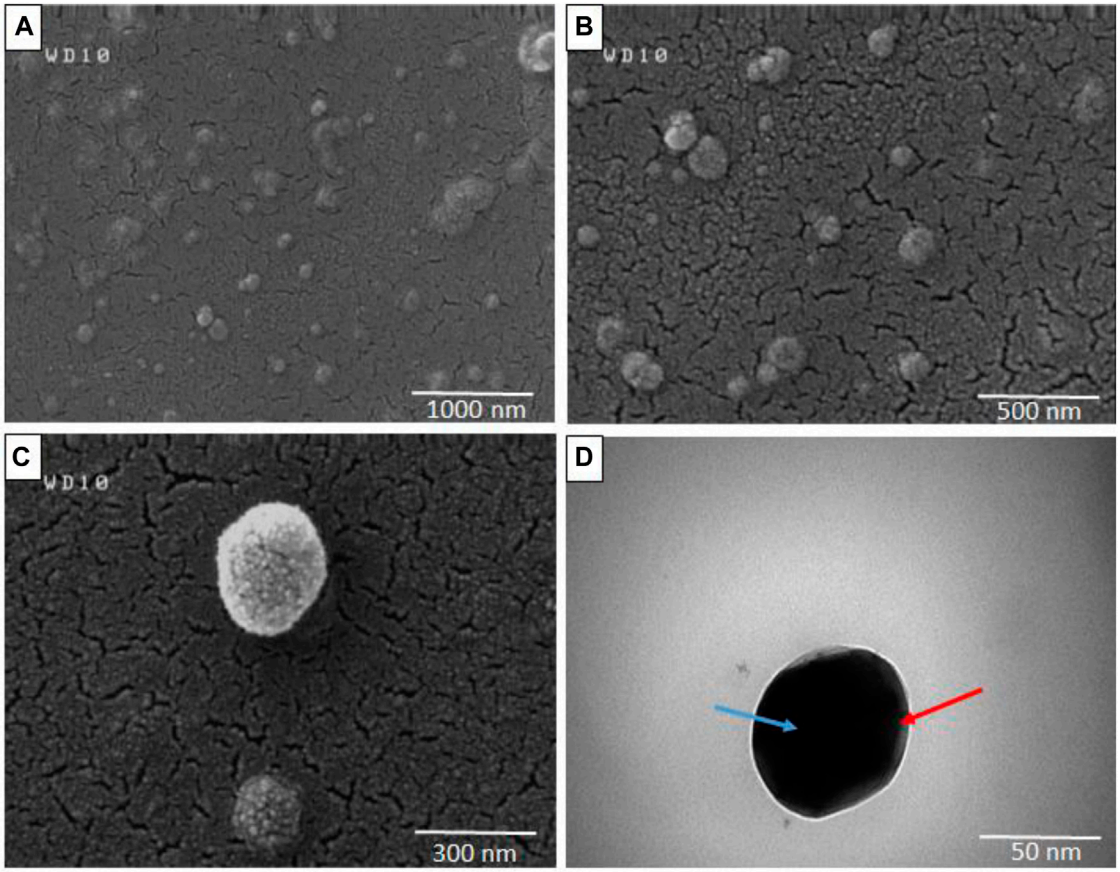

FIGURE 5
Field emission scanning electron microscopy (FESEM) **(A–C)** and Transmission electron microscopy (TEM) **(D)** of Polymeric micelles in different resolutions (Blue arrow: micelle core, Red arrow: micelle shell).

Under analysis conditions of 15.0 kV accelerating voltage, 500.0 pA beam current, and 5,000 magnification, EDX spectroscopy and elemental mapping analysis was conducted on PM-Ag. The results have been presented in Figures 6A–E. Additionally, the UV-vis spectroscopy pertaining to both the PM and PM-Ag samples is illustrated in Figure 6F.

3.3 Clotrimazole release study

The release profile of clotrimazole was investigated in a 10 mM PBS/ethanol medium with pH 7.3 and a constant temperature of 37°C. At predetermined intervals, the entire release medium was buffer exchanged, and the sample's UV-vis absorption was measured at a wavelength of 230 nm. Unknown concentrations were then calculated using the Clt standard curve equation. Ethanol was added to the release medium to maintain the sink release condition. A diagram displaying the cumulative Clt release from PM-Clt solution over 6 days at pH 7.3°C and 37 °C is shown in Figure 7.

3.4 Cytotoxicity of the micelles

The impact of PM, PM-Ag, PM-Clt, PM-Clt-Ag, and H-PM-Clt-Ag on HEK293 cells was examined to assess its cytotoxicity. Figure 8 displays the viability of HEK293 cells after being cultivated with varying concentrations of micelles for 48 h. The results indicate that up to a concentration of 125 μg/mL, the relative cell viability percentage exceeded 80%. This suggests remarkably low toxicity levels of micelles against mammalian cells.

3.5 Antifungal activity

The evaluation of polymeric micelles' antifungal properties was conducted utilizing *Candida* albicans. The fungal cells were exposed to distinct concentrations of the solution which were then incubated at a temperature of 35 °C for 48 h Subsequently, using UV-vis spectrophotometry, the optical density of fungal cell growth was determined at 530 nm. Figure 9 illustrates the viability percentages of fungal cells that underwent various concentrations of five types of samples, namely, PM, PM-Ag, PM-Clt, PM-Clt-Ag, and H-PM-Clt-Ag.

4 Discussion

The FTIR spectrum of LGL reveals four absorption bands that provide important information about the chemical groups present in

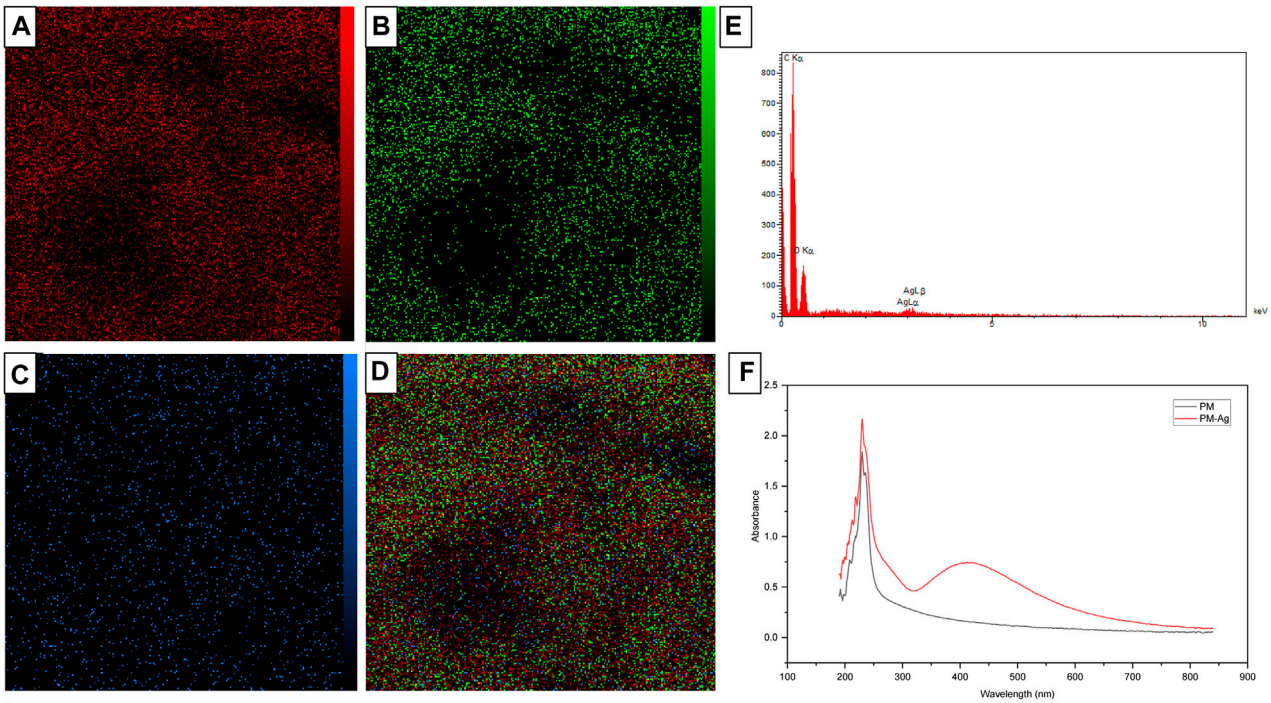

FIGURE 6
Energy-dispersive X-ray spectroscopy **(E)** and elemental mapping of Silver-beared polymeric micelles displaying carbon **(A)**, oxygen **(B)**, silver elements **(C)**, and the combined one **(D)**, besides UV-vis spectroscopy of Polymeric micelles and Silver-beared polymeric micelles **(F)**.

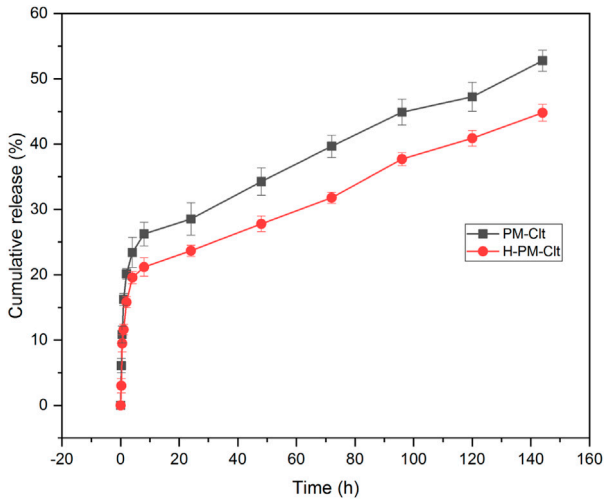

FIGURE 7
Cumulative release profile of Clotrimazole-loaded polymeric micelles (PM-Clt) and Hydrogel containing clotrimazole-loaded micelles (H-PM-Clt) in 10 mM PBS/ethanol at pH 7.3.

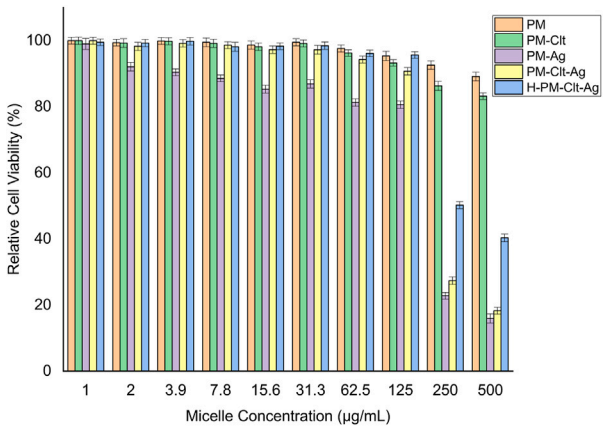

FIGURE 8
Relative cell viability percentage of HEK293 cells against PM, PM-Clt, PM-Ag, PM-Clt-Ag, and H-PM-Clt-Ag after 48 h of incubation at various concentrations of 1, 2, 3.9, 7.8, 15.6, 31.3, 62.5, 125, 250, and 500 μg/mL. Normal saline was used in the control group. Data were presented as mean ± SD, n = 3.

the sample. An absorption band appearing at a wavelength of approximately 1723 cm^{-1} corresponds to the ester carbonyl group (C=O) of ε-caprolactone, while the absorption band observed at 1,105 cm^{-1} corresponds to the PEG -OCH_2CH_2 repeating units. Additionally, two absorption bands appear at wavelengths of around 1,240 and 3,620 cm^{-1}, which belong to the -COO- bands and terminal hydroxyl groups of PCL, respectively.

The FTIR spectrum of GLG displays an absence of absorption within the 2,270–2,250 cm^{-1} range. This lack of absorption establishes the complete disappearance of hexamethylene diisocyanate -NCO groups.

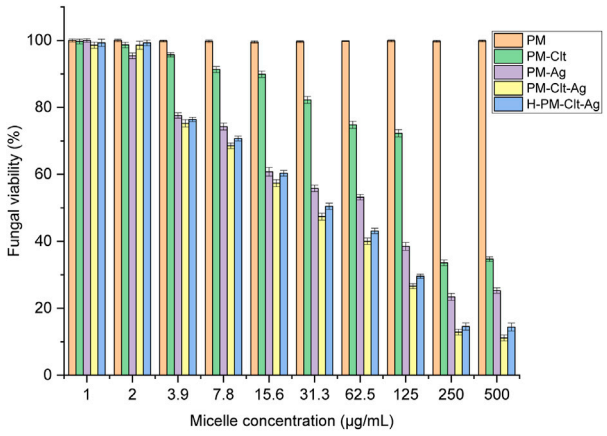

FIGURE 9
Fungal viability of five Polymeric micelles (PM, PM-Clt, PM-Ag, PM-Clt-Ag, and H-PM-Clt-Ag) after 48 h of incubation at 35°C, at various concentrations of 1, 2, 3.9, 7.8, 15.6, 31.3, 62.5, 125, 250, and 500 μg/mL. Positive control: (medium + fungal suspension), negative control: (medium). Data were presented as mean ± SD, $n = 3$.

Such disappearance is attributed to a coupling reaction between the -NCO and -OH groups. Moreover, the absorption band observed at 1,527 cm^{-1} can be attributed to the N-H group which demonstrates the formation of tri-block copolymers. Thus, the accuracy of tri-block copolymer synthesis is confirmed by the FTIR spectrum. Additionally, the copolymer formation and the number-average molecular weight determination of copolymers were further confirmed through the use of HNMR spectrum. The LGL HNMR spectrum shows several peaks corresponding to different methylene protons in the copolymer. Specifically, the peak at 1.4 ppm and 1.65 ppm are related to -$(CH_2)_3$- methylene protons, while the peak at 2.32 ppm is associated with -$OCCH_2$- methylene protons. Additionally, the peak at 4.06 ppm corresponds to -CH_2OOC- methylene protons in PCL units, and the higher intensity peak at 3.65 ppm is attributed to -CH_2CH_2O- methylene protons in PEG units. Moreover, short peaks at 3.82 and 4.23 ppm refer to -O-CH_2-CH_2- methylene protons in the PCL blocks' PEG terminal units. In contrast, the GLG HNMR spectrum displays peaks at 3.6 and 3.38 ppm referring to -CH_2CH_2O- and terminal groups -OCH_3 in the PEG blocks, respectively. Similarly, the peaks at 1.35 and 1.62 ppm correspond to -$(CH_2)_3$- methylene protons, and the peak at 2.3 ppm correlates with -$OCCH_2$- methylene protons. Furthermore, the peak at 4.06 ppm corresponds to -CH_2OOC- methylene protons of PCL units, and the short peaks at 4.20 and 3.82 ppm relate to O-CH_2-CH_2- methylene protons of PEG terminal unit attached to the PCL blocks. Finally, GPC analysis was utilized to determine the M_n, M_w, and polydispersity of copolymers. Table 2 presents a comprehensive summary of all the results obtained. The PCL/PEG ratio of copolymers was calculated using the HNMR spectrum, which revealed a ratio of 1.54:1 and 2.32:1 for LGL and GLG copolymers respectively. The values obtained through experimentation exhibit a degree of similarity to the corresponding feeding ratios presented in Table 1. However, they are not entirely identical due to the derivation of the data in Table 1 being based on theoretical assumptions. On the other hand, the values calculated above are derived from actual experimental results. Consequently, we can draw the conclusion that the experimental data aligns with the anticipated values, thus confirming the accuracy of the conducted analysis.

PCL has a negative surface charge that can be mitigated by the addition of neutral PEG blocks, leading to less negative values of total zeta potential (Cu et al., 2011; Suk et al., 2016). Figure 3 demonstrates that the zeta potential results of the PM solution at pH 7.3 revealed a negative surface charge of the micelles, indicating that the adsorption of silver ions on the micelles was caused by the electrostatic interaction between positively charged ions and negatively charged micelles. When silver nitrate solution was added to the PM solution, Ag^+ ions were adsorbed to the negative surface of the PM. Subsequently, the introduction of sodium borohydride to the solution resulted in the reduction of the silver ions, ultimately leading to the development of silver nanoparticles on the polymeric micelles. The yellowish color illustrated in Figure 1 confirms the accuracy of the reduction of silver ions. The presented FTIR spectrum in Figure 4A pertaining to clotrimazole drug indicates several absorption bands, each occurring at specific wavelengths. In particular, the absorption bands found at the wavelengths 753.07, 822.49, 904.45, 1208.18, and 1273.75 cm^{-1} signify the bending vibration of C-H bonds, while those at 1040.41 and 1079.94 cm^{-1} correspond to the stretching vibration of C-N bonds in the aromatic ring of imidazole. Similarly, the absorption band at the wavelength of 1438.64 cm^{-1} denotes the stretching vibration of the C=C bond of the aromatic ring of imidazole, whereas the absorption band occurring at 1592.91 cm^{-1} signifies the stretching vibration of the C=N bond in the aromatic ring of imidazole. The absorption band that appears at the wavelength of 3055.66 cm^{-1} corresponds to the stretching vibration of the C-H bond in the aromatic ring. In Figures 4B, a comparison between the FTIR spectra of clotrimazole, blank micelle, and clotrimazole-loaded micelle is presented. Notably, the absorption bands of clotrimazole and polymer present in the clotrimazole-loaded micelle demonstrate that the Clt has indeed been loaded in the polymeric micelle. The average size of PMs, as determined by ImageJ software and depicted in Figure 5, closely aligns with the findings from dynamic light scattering (DLS). Moreover, the accurate representation of the micelles' morphological structure was observed.

The EDX spectroscopy and elemental mapping analysis depicted in Figures 6A–E reveals the presence of oxygen, carbon, and silver elements in the structure of PM-Ag. PEG-PCL polymeric micelles are primarily composed of carbon and oxygen, which is confirmed by the higher peak intensity of these two elements. Additionally, the existence of silver in the PM-Ag structure is supported by peak observation at an energy of about 3 kV. Comparing the UV-vis spectroscopy of the PM and PM-Ag (Figure 6F), it is evident that the special peak at 410 nm related to the surface plasmon resonance of silver nanoparticles confirms the presence of silver in the PM-Ag solution.

The micelles exhibited an encapsulation efficiency of 64.53% and a drug loading of 14.6%. Figure 7 shows that the drug release profile from H-PM-Clt is similar to that of the PM-Clt solution, with a lower total percentage of drug release observed in the hydrogel. Specifically, PM-Clt had a total percentage of drug release of 53%, while H-PM-Clt had a total percentage of 44.8%. The similarity in the slopes of the two graphs indicates that the drug release rates for both samples were almost identical.

Polymeric micelles have a unique characteristic of penetrating fungal cells through endocytosis and acting as a delivery vehicle for drugs into the cells which enhances their pharmacological activity (Nelemans and Gurevich, 2020). As shown in Figure 8, the viability of cells remains high, exceeding 80%, when micelle concentration is at or below 125 μg/mL. Nevertheless, as the concentration of

TABLE 2 M_n, M_w, and polydispersity of copolymers.

Sample	M_n[a]	M_n[b]	M_n[c]	M_w[c]	Pd (M_w[c]/M_n[c])
LGL	16,000	15,268	15,393	20,293	1.32
GLG	3,300	3,656	2,253	4,132	1.83

Pd, polydispersity (M_w/M_n). a, Feeding ratio; b, Calculated from HNMR results; c, Calculated from GPC results.

micelles rises beyond this threshold, there is an observable rise in cytotoxicity levels. In the control group, the cell viability was 100%. In a similar study, the toxicity effect of Ag-decorated MPEG-g-PU vesicles on HUVEC cells was performed and the results displayed that by concentration rising of silver nanoparticles, the cell viability decreases which at 20 μg/mL of silver concentration the cell viability declined to 72% while this concentration is much higher than the MIC and MBC of designated micelles. In Huang et al.'s study, silver-decorated curcumin-loaded Poly(aspartic acid)-PCL polymeric micelles showed very low toxicity to mammalian cells across all investigated concentrations (Huang et al., 2017; Su et al., 2017).

In Figure 9, it is demonstrated that pure PM is not effective against fungi at any concentration considered. However, the viability of fungal cells decreases as the concentration of PM-Ag and PM-Clt increases. The growth inhibition of PM-Ag is more pronounced than PM-Clt, but PM-Clt-Ag displays a synergistic effect in inhibiting the growth of *Candida* albicans cells. The antifungal activity of H-PM-Clt-Ag is less than PM-Clt-Ag but higher than PM-Clt and PM-Ag. According to Section 3.3, the comparison chart of PM-Clt and H-PM-Clt indicates that loading polymeric micelles into hydrogels leads to a significant decrease in drug release rate. Therefore, H-PM-Clt-Ag exhibits lower antifungal activity when compared to the PM-Clt-Ag sample. As shown in Figures 8, 9, at 125 μg/mL concentration the cell viability and fungal viability of H-PM-Clt-Ag were approximately 95% and 30% respectively. At 250 μg/mL concentration, the cell viability was reduced to 50% and fungal viability reached 15%. Depending on the severity of the disease, the physician determines that losing several healthy cells to provide more effective treatment will be the preferable way of healing. The antibacterial potential of Ag-decorated MPEG-g-PU vesicles against *E. coli* and *S. aureus* bacteria examined by Su et al. revealed that concentrations of 5.24 and 10.48 μg/mL of Ag produced the greatest inhibition of growth. However, when compared to PM-Ag, PM-Clt-Ag, and H-PM-Clt-Ag, which exhibited 28.5, 26.4, and 22.9 μg/mL of silver content at 125 μg/mL concentration of micelle measured by ICP, it becomes apparent that higher levels of silver are necessary to achieve the desired antifungal activity. Huang's study demonstrated that the bacterial viability of silver-decorated curcumin-loaded Poly(aspartic acid)-PCL polymeric micelles at 125 μg/mL concentration of the micelle was approximately 45% against *S. aureus* and 40% against *P. aeruginosa*. However, the current research study provides evidence for a higher level of effectiveness in terms of antifungal activity (Huang et al., 2017; Su et al., 2017).

5 Conclusion

To summarize this study, a core/shell polymeric micelle containing clotrimazole and silver nanoparticles was developed and demonstrated significant antifungal activity against *Candida* albicans. The combination of clotrimazole and silver nanoparticles had a synergistic effect, enhancing the antifungal properties of the drug delivery system. Additionally, the silver-beared polymeric micelles were found to be cytocompatible with HEK293T cells at certain concentrations. These results suggest that a thermosensitive hydrogel system loaded with silver-beared polymeric micelles with desirable properties may be suitable for treating vaginal candidiasis.

Data availability statement

The original contributions presented in the study are included in the article/Supplementary Material, further inquiries can be directed to the corresponding author.

Author contributions

FH designed and conducted the experiments for this study and wrote the original manuscript. HT supervised the study and edited the manuscript. FF proposed the idea and cosupervised the study. All authors contributed to the article and approved the submitted version.

Funding

This project was funded by the Preventative Gynecology Research Center (PGRC) with contract number 01-20069 and the ethical committee approval code of IR.SBMU.RETECH.REC.1400.868.

Acknowledgments

Scientific and financial support of PGRC is gratefully acknowledged. The collaborations of the staff of the chemical/biomedical Engineering laboratory at the Department of Life Science Engineering, Faculty of New Sciences and Technologies, University of Tehran are also acknowledged.

Conflict of interest

The authors declare that the research was conducted in the absence of any commercial or financial relationships that could be construed as a potential conflict of interest.

Publisher's note

References

Abdellatif, M. M., Khalil, I. A., Elakkad, Y. E., Eliwa, H. A., Samir, T. M., and Al-Mokaddem, A. K. (2020). Formulation and characterization of sertaconazole nitrate mucoadhesive liposomes for vaginal candidiasis. *Int. J. Nanomedicine* 15, 4079–4090. doi:10.2147/ijn.s250960

Albayaty, Y. N., Thomas, N., Ramírez-García, P. D., Davis, T. P., Quinn, J. F., Whittaker, M. R., et al. (2021). Polymeric micelles with anti-virulence activity against Candida albicans in a single-and dual-species biofilm. *Drug Deliv. Transl. Res.* 11, 1586–1597. doi:10.1007/s13346-021-00943-4

Biswas, S., Kumari, P., Lakhani, P. M., and Ghosh, B. (2016). Recent advances in polymeric micelles for anti-cancer drug delivery. *Eur. J. Pharm. Sci.* 83, 184–202. doi:10.1016/j.ejps.2015.12.031

Brandolt, T. M., Klafke, G. B., Gonçalves, C. V., Bitencourt, L. R., Martinez, A. M. B. D., Mendes, J. F., et al. (2017). Prevalence of Candida spp. in cervical-vaginal samples and the *in vitro* susceptibility of isolates. *Braz. J. Microbiol.* 48, 145–150. doi:10.1016/j.bjm.2016.09.006

Cabral, H., Miyata, K., Osada, K., and Kataoka, K. (2018). Block copolymer micelles in nanomedicine applications. *Chem. Rev.* 118, 6844–6892. doi:10.1021/acs.chemrev.8b00199

Cassano, R., Ferrarelli, T., Mauro, M. V., Cavalcanti, P., Picci, N., and Trombino, S. (2016). Preparation, characterization and *in vitro* activities evaluation of solid lipid nanoparticles based on PEG-40 stearate for antifungal drugs vaginal delivery. *Drug Deliv.* 23, 1037–1046. doi:10.3109/10717544.2014.932862

Catenacci, L., Marrubini, G., Sorrenti, M., Rossi, S., Sandri, G., Ferrari, F., et al. (2020). Design of experiments-assisted development of clotrimazole-loaded ionic polymeric micelles based on hyaluronic acid. *Nanomaterials* 10, 635. doi:10.3390/nano10040635

Cu, Y., Booth, C. J., and Saltzman, W. M. (2011). *In vivo* distribution of surface-modified PLGA nanoparticles following intravaginal delivery. *J. Control. release* 156, 258–264. doi:10.1016/j.jconrel.2011.06.036

Das Neves, J., Nunes, R., Machado, A., and Sarmento, B. (2015). Polymer-based nanocarriers for vaginal drug delivery. *Adv. drug Deliv. Rev.* 92, 53–70. doi:10.1016/j.addr.2014.12.004

Ensign, L. M., Cone, R., and Hanes, J. (2014). Nanoparticle-based drug delivery to the vagina: A review. *J. Control. Release* 190, 500–514. doi:10.1016/j.jconrel.2014.04.033

Facchinatto, W. M., Galante, J., Mesquita, L., Silva, D. S., Dos Santos, D. M., Moraes, T. B., et al. (2021). Clotrimazole-loaded N-(2-hydroxy)-propyl-3-trimethylammonium, O-palmitoyl chitosan nanoparticles for topical treatment of vulvovaginal candidiasis. *Acta biomater.* 125, 312–321. doi:10.1016/j.actbio.2021.02.029

Frank, L. A., Chaves, P. S., D'amore, C. M., Contri, R. V., Frank, A. G., Beck, R. C., et al. (2017). The use of chitosan as cationic coating or gel vehicle for polymeric nanocapsules: Increasing penetration and adhesion of imiquimod in vaginal tissue. *Eur. J. Pharm. Biopharm.* 114, 202–212. doi:10.1016/j.ejpb.2017.01.021

Gong, C., Qian, Z., Liu, C., Huang, M., Gu, Y., Wen, Y., et al. (2007). A thermosensitive hydrogel based on biodegradable amphiphilic poly (ethylene glycol)–polycaprolactone–poly (ethylene glycol) block copolymers. *Smart Mater. Struct.* 16, 927–933. doi:10.1088/0964-1726/16/3/043

Gou, M. L., Qian, Z. Y., Wang, H., Tang, Y. B., Huang, M. J., Kan, B., et al. (2008). Preparation and characterization of magnetic poly (ε-caprolactone)-poly (ethylene glycol)-poly (ε-caprolactone) microspheres. *J. Mater. Sci. Mater. Med.* 19, 1033–1041. doi:10.1007/s10856-007-3230-3

Gou, M., Zheng, L., Peng, X., Men, K., Zheng, X., Zeng, S., et al. (2009). Poly (ε-caprolactone)–poly (ethylene glycol)–poly (ε-caprolactone)(PCL–PEG–PCL) nanoparticles for honokiol delivery *in vitro*. *Int. J. Pharm.* 375, 170–176. doi:10.1016/j.ijpharm.2009.04.007

Grossen, P., Witzigmann, D., Sieber, S., and Huwyler, J. (2017). PEG-PCL-based nanomedicines: A biodegradable drug delivery system and its application. *J. Control. Release* 260, 46–60. doi:10.1016/j.jconrel.2017.05.028

Huang, F., Gao, Y., Zhang, Y., Cheng, T., Ou, H., Yang, L., et al. (2017). Silver-decorated polymeric micelles combined with curcumin for enhanced antibacterial activity. *ACS Appl. Mater. interfaces* 9, 16880–16889. doi:10.1021/acsami.7b03347

Hwang, D., Ramsey, J. D., and Kabanov, A. V. (2020). Polymeric micelles for the delivery of poorly soluble drugs: From nanoformulation to clinical approval. *Adv. drug Deliv. Rev.* 156, 80–118. doi:10.1016/j.addr.2020.09.009

Johal, H. S., Garg, T., Rath, G., and Goyal, A. K. (2016). Advanced topical drug delivery system for the management of vaginal candidiasis. *Drug Deliv.* 23, 550–563. doi:10.3109/10717544.2014.928760

Kareem, F., Bhayo, A. M., Imran, M., Shah, M. R., Khan, K. M., and Malik, M. I. (2019). Enhanced therapeutic efficacy of clotrimazole by delivery through poly (ethylene oxide)-block-poly (ε-caprolactone) copolymer-based micelles. *J. Appl. Polym. Sci.* 136, 47769. doi:10.1002/app.47769

Kim, M. S., Seo, K. S., Khang, G., Cho, S. H., and Lee, H. B. (2004). Preparation of methoxy poly (ethylene glycol)/polyester diblock copolymers and examination of the gel-to-sol transition. *J. Polym. Sci. Part A Polym. Chem.* 42, 5784–5793. doi:10.1002/pola.20430

Lee, S. H., and Jun, B.-H. (2019). Silver nanoparticles: Synthesis and application for nanomedicine. *Int. J. Mol. Sci.* 20, 865. doi:10.3390/ijms20040865

Li, Y., Huang, W., Li, Y., Chiu, W., and Cui, Y. (2020). Opportunities for cryogenic electron microscopy in materials science and nanoscience. *ACS nano* 14, 9263–9276. doi:10.1021/acsnano.0c05020

Lombardo, D., Kiselev, M. A., and Caccamo, M. T. (2019). Smart nanoparticles for drug delivery application: Development of versatile nanocarrier platforms in biotechnology and nanomedicine. *J. Nanomater.* 2019, 1–26. doi:10.1155/2019/3702518

Lombardo, D., Kiselev, M. A., Magazù, S., and Calandra, P. (2015). Amphiphiles self-assembly: Basic concepts and future perspectives of supramolecular approaches. *Adv. Condens. Matter Phys.* 2015, 1–22. doi:10.1155/2015/151683

Mikhailova, E. O. (2020). Silver nanoparticles: Mechanism of action and probable bio-application. *J. Funct. biomaterials* 11, 84. doi:10.3390/jfb11040084

Miyata, K., Christie, R. J., and Kataoka, K. (2011). Polymeric micelles for nano-scale drug delivery. *React. Funct. Polym.* 71, 227–234. doi:10.1016/j.reactfunctpolym.2010.10.009

Nelemans, L. C., and Gurevich, L. (2020). Drug delivery with polymeric nanocarriers—Cellular uptake mechanisms. *Materials* 13, 366. doi:10.3390/ma13020366

Nogueira, N. C., De Sá, L. L. F., and De Carvalho, A. L. M. (2022). Nanostructured lipid carriers as a novel strategy for topical antifungal therapy. *AAPS PharmSciTech* 23, 32–10. doi:10.1208/s12249-021-02181-w

Panáček, A., Kolář, M., Večeřová, R., Prucek, R., Soukupova, J., Kryštof, V., et al. (2009). Antifungal activity of silver nanoparticles against Candida spp. *Biomaterials* 30, 6333–6340. doi:10.1016/j.biomaterials.2009.07.065

Santos, S. S., Lorenzoni, A., Ferreira, L. M., Mattiazzi, J., Adams, A. I., Denardi, L. B., et al. (2013). Clotrimazole-loaded Eudragit® RS100 nanocapsules: Preparation, characterization and *in vitro* evaluation of antifungal activity against Candida species. *Mater. Sci. Eng. C* 33, 1389–1394. doi:10.1016/j.msec.2012.12.040

Santos, S. S., Lorenzoni, A., Pegoraro, N. S., Denardi, L. B., Alves, S. H., Schaffazick, S. R., et al. (2014). Formulation and *in vitro* evaluation of coconut oil-core cationic nanocapsules intended for vaginal delivery of clotrimazole. *Colloids Surfaces B Biointerfaces* 116, 270–276. doi:10.1016/j.colsurfb.2014.01.011

Soriano-Ruiz, J. L., Calpena-Capmany, A. C., Cañadas-Enrich, C., Bozal-De Febrer, N., Suñer-Carbó, J., Souto, E. B., et al. (2019). Biopharmaceutical profile of a clotrimazole nanoemulsion: Evaluation on skin and mucosae as anticandidal agent. *Int. J. Pharm.* 554, 105–115. doi:10.1016/j.ijpharm.2018.11.002

Su, Y., Zhao, L., Meng, F., Wang, Q., Yao, Y., and Luo, J. (2017). Silver nanoparticles decorated lipase-sensitive polyurethane micelles for on-demand release of silver nanoparticles. *Colloids Surfaces B Biointerfaces* 152, 238–244. doi:10.1016/j.colsurfb.2017.01.036

Suk, J. S., Xu, Q., Kim, N., Hanes, J., and Ensign, L. M. (2016). PEGylation as a strategy for improving nanoparticle-based drug and gene delivery. *Adv. drug Deliv. Rev.* 99, 28–51. doi:10.1016/j.addr.2015.09.012

Takahashi, C., Yamada, T., Yagi, S., Murai, T., and Muto, S. (2021). Preparation of silver-decorated Soluplus® nanoparticles and antibacterial activity towards S. epidermidis biofilms as characterized by STEM-CL spectroscopy. *Mater. Sci. Eng. C* 121, 111718. doi:10.1016/j.msec.2020.111718

Taurin, S., Almomen, A. A., Pollak, T., Kim, S. J., Maxwell, J., Peterson, C. M., et al. (2018). Thermosensitive hydrogels a versatile concept adapted to vaginal drug delivery. *J. drug Target.* 26, 533–550. doi:10.1080/1061186x.2017.1400551

Tonglairoum, P., Woraphatphadung, T., Ngawhirunpat, T., Rojanarata, T., Akkaramongkolporn, P., Sajomsang, W., et al. (2017). Development and evaluation of N-naphthyl-N, O-succinyl chitosan micelles containing clotrimazole for oral candidiasis treatment. *Pharm. Dev. Technol.* 22, 184–190. doi:10.3109/10837450.2016.1163391

Wei, X., Gong, C., Gou, M., Fu, S., Guo, Q., Shi, S., et al. (2009). Biodegradable poly (ε-caprolactone)–poly (ethylene glycol) copolymers as drug delivery system. *Int. J. Pharm.* 381, 1–18. doi:10.1016/j.ijpharm.2009.07.033

Willems, H. M. E., Ahmed, S. S., Liu, J., Xu, Z., and Peters, B. M. (2020). Vulvovaginal candidiasis: A current understanding and burning questions. *J. Fungi* 6, 27. doi:10.3390/jof6010027

Nomenclature

Clt	Clotrimazole
LGL	PCL-PEG-PCL
GLG	PEG-PCL-PEG
PM	Polymeric micelles
PM-Clt	Clotrimazole-loaded polymeric micelles
PM-Ag	Silver-beared polymeric micelles
PM-Clt-Ag	Clotrimazole-loaded Ag micelles
H-PM-Clt-Ag	Hydrogel containing clotrimazole-loaded Ag micelles